Nonlocal Effects in the Plasmons of Strongly Interacting Nanoparticles, Dimers, and Waveguides

F. Javier García de Abajo*

Instituto de Óptica−CSIC, Serrano 121, 28006 Madrid, Spain

Received: August 16, 2008; Revised Manuscript Received: September 4, 2008

Spatial nonlocality in the optical response of noble metals is shown to produce significant blue shift and near-field quenching of plasmons in nanoparticle dimers, nanoshells, and thin metal waveguides. Compared with a local description relying on the use of frequency-dependent dielectric functions, we predict resonance shifts as large as 10% and field-intensity reduction of an order of magnitude at interparticle distances or metal thicknesses below 2 Å, although sizable effects are already observed for dimers separated by 2 nm. The calculation method (a combination of the specular-reflection model and a suitable nonlocal extension of measured local dielectric functions) is simple to implement and can be easily generalized to arbitrarily complex nanostructures.

I. Introduction

Knowledge of the optical response of materials at the nanoscale has become a pillar of nanophotonics. While excellent agreement between theory and experiment is generally achieved for nanoparticles and nanostructured materials by relying on local, frequency-dependent dielectric functions,[1,2] nonlocal effects are known to play an important role at small distances in the nanometer region.[3] In particular, quantum-confinement effects lead to significant plasmon broadening in metallic nanoparticles of diameter below 10 nm.[3] This range of distances is becoming experimentally feasible in metallic dimers,[4] nanoshells,[5] and tips,[6] which exhibit large near-field enhancement[7,8] with practical application to improved SERS biosensing,[9,6] photovoltaics,[10] and solid-state lighting.[11] However, no account of nonlocal effects has been reported in such systems, due in part to the complexity of nonlocal descriptions of the optical response in inhomogeneous environments.

First-principles calculations of the optical response are only available for relatively simple systems, such as bulk metals and clusters of up to hundreds of noble metal atoms,[12] which are insufficient to describe larger nanoparticles (e.g., ∼250000 atoms in the 20-nm Au particles considered below). However, several approximate prescriptions have been elaborated to deal with more complicated systems, and most notably the *d*-function formalism of Feibelman[13] and the specular reflection model (SRM).[14−16] The latter is particularly advantageous because it permits expressing the response of bounded homogeneous media in terms of their nonlocal bulk dielectric function, as already reported in studies of fast electrons and ions moving near planar surfaces.[17]

Here, we carry out SRM calculations of dimers, shells, and thin waveguides made of gold and silver. We show that nonlocal effects produce significant plasmon blue shifts and reduction of the near-field enhancement. The response is constructed from measured optical constants, which are extended to include nonlocal effects in the contribution of valence electrons. The validity of this model is corroborated by successfully explaining experimentally observed quantum-confinement effects, which lead to broadening and blue shift of plasmons in small metal particles. We draw conclusions on more complicated systems of relevance in plasmonics by applying the same model and establish a computational procedure to be applied to arbitrarily complex geometries.

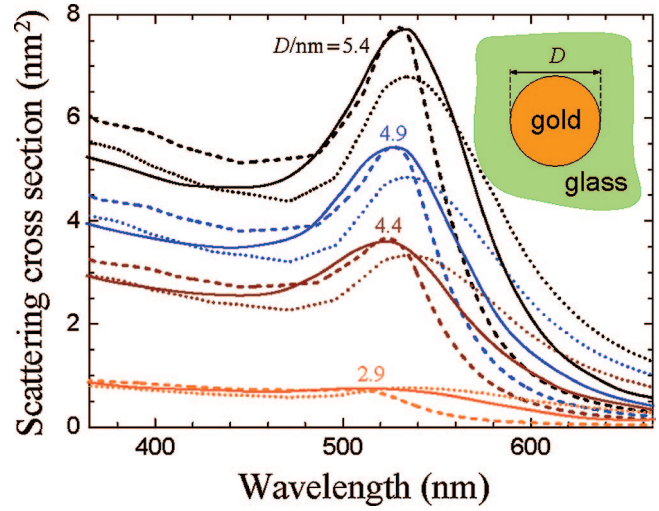

Figure 1. Extinction spectra of spherical gold particles embedded in glass ($\epsilon = 2.3$). Experimental spectra taken from ref 3 (solid curves) are compared here with the phenomenological theory of eq 1 (dotted curves) and the present nonlocal theory (dashed curves) for various values of the particle diameter (see text insets).

Nonlocal effects have been long realized to produce significant plasmon broadening in small noble metal nanocrystals,[3] as shown in Figure 1 for spherical gold particles. The plasmon resonance is drastically reduced as the particle size decreases to a value close to the mean free path of excited electrons in the vicinity of the Fermi level. These so-called finite-size effects have been phenomenologically accounted for by increasing the damping rate of the conduction electrons contribution to the permittivity,[3] so that the particle is described through the modified dielectric function

$$\epsilon(q,\omega) = \epsilon^{\mathrm{loc}}(\omega) + \omega_p^2/\omega(\omega + i\eta) - \omega_p^2/\omega(\omega + i\eta + iv_F/a) \quad (1)$$

where $\epsilon^{\mathrm{loc}}(\omega)$ is the local, frequency-dependent part of the response, which we take from optical measurements performed

* Electronic address: jga@cfmac.csic.es.

10.1021/jp807345h CCC: $40.75
Published on Web 10/24/2008

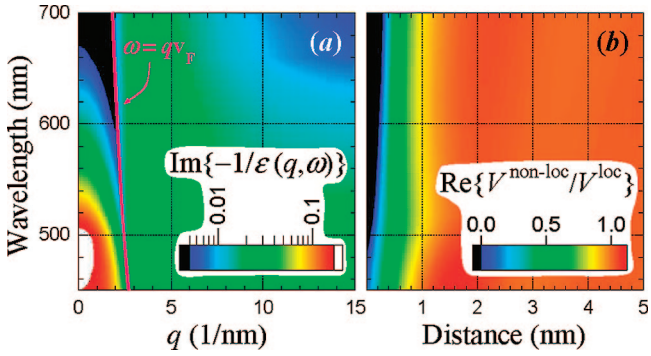

Figure 2. (a) Nonlocal wavelength- and momentum-dependent response function of homogeneous gold. (b) Distance dependence of the nonlocal interaction potential derived from part a and normalized to the local potential $1/[r\epsilon^{\mathrm{loc}}(\omega)]$.

on extended planar surfaces,[18] ω_p and η are the valence-electron-gas plasma frequency and the plasmon width of the bulk metal, respectively, v_F is the Fermi velocity, and a is the particle radius. In other words, the damping rate η in the conduction electron motion is increased by the rate of collisions (v_F/a) with the particle surface for electrons moving near the Fermi level (i.e., those actually determining the collective plasmon response). This procedure brings theory into reasonable agreement with experiment, as shown in Figure 1 (solid and dotted curves represent experiment and phenomenological theory, respectively), using parameter values $\hbar\omega_p = 9$ eV, $\hbar\eta = 0.05$ eV, and $v_F = 1.39 \times 10^8$ cm/s, appropriate for gold, and it is quite different from the nearly size-independent spectral profile predicted without finite-size corrections for small a.[19] It should be noted however that the recipe just outlined is not so well defined for nonspherical particles (or even for shells, in which the distance traveled by conduction electrons before they hit a metal boundary is not solely determined by the radius but also by the shell thickness). Furthermore, nonlocal effects are expected to play a significant role in sharp corners of bigger particles, but no methods are currently available to successfully describe these situations. Some of these geometries are considered in this work, and a general procedure to calculate nonlocal effects in all of them is explained, which results in a reasonable, parameter-free description of spherical particles as well (dashed curves in Figure 1).

II. Nonlocal Effects in Homogeneous Media

In the local approximation, the electric displacement $\mathbf{D}(\mathbf{r},\omega)$ depends on the electric field $\mathbf{E}(\mathbf{r},\omega)$ only at the same position $\mathbf{r}$ through

$$\mathbf{D}(\mathbf{r},\omega) = \epsilon(\mathbf{r},\omega)\mathbf{E}(\mathbf{r},\omega)$$

where $\epsilon(\mathbf{r},\omega)$ is the space- and frequency-dependent local dielectric function. In contrast, nonlocal media exhibit a general dependence as

$$\mathbf{D}(\mathbf{r},\omega) = \int d\mathbf{r}'\ \epsilon(\mathbf{r},\mathbf{r}',\omega)\mathbf{E}(\mathbf{r}',\omega) \qquad (2)$$

where $\epsilon(\mathbf{r}, \mathbf{r}',\omega)$ gives the nonlocal response. We can seek inspiration on how to include nonlocal effects in nanostructured materials by first examining the case of homogeneous media, for which $\epsilon(\mathbf{r}, \mathbf{r}',\omega)$ is a function of $\mathbf{r} - \mathbf{r}'$. Then, the convolution of eq 2 reduces to the algebraic relation

$$\mathbf{D}(q,\omega) = \epsilon(\mathbf{q},\omega)\mathbf{E}(\mathrm{q},\omega)$$

in momentum space $\mathbf{q}$, related to real space via Fourier transformation.

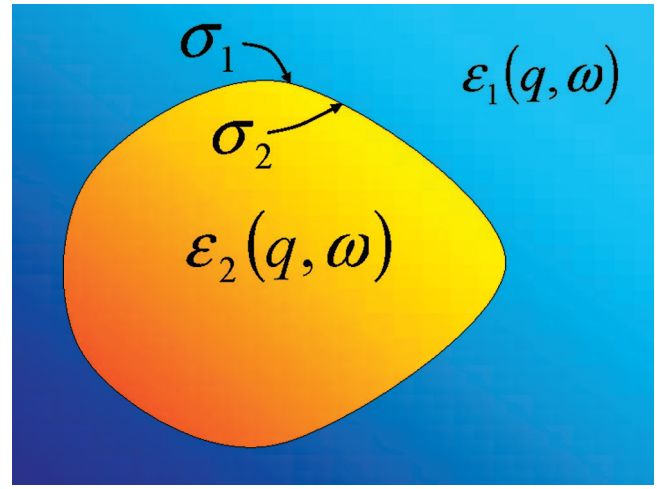

Figure 3. Implementation of the specular reflection model (SRM). This model incorporates nonlocality by describing each media outside and inside an interface through their corresponding momentum-dependent homogeneous dielectric functions $\epsilon_j(q,\omega)$. The electric potential is solved within each medium j (treated as infinite and homogeneous) in the presence of external charges within that medium plus a boundary charge distribution σ_j. These boundary charges are used to impose the continuity of the potential and the normal displacement. This procedure was proposed to derive simple expressions for the nonlocal surface-plasmon dispersion relation,[14,15] and it can be traced back to the random-phase approximation of the system, with the boundaries described as infinite barrier toward conduction electrons and after neglecting quantum interference between free electrons and their reflection at the surface.[25]

In general, insulators behave as local media, whereas delocalized s valence electrons in noble metals constitute a source of nonlocality. It is thus reasonable to treat the response of both insulators and core-polarization in metals as local, and to approximate the valence-electron contribution in the $q \to 0$ limit by the Drude formula

$$\epsilon^{\mathrm{D}}(\omega) = 1 - \omega_p^2/\omega(\omega + i\eta)$$

where ω_p and η are as in eq 1. Delocalized valence excitations produce a significant q dependence, as studied by Lindhard in the so-called random-phase approximation (RPA)[20] and later by Mermin to include electron-motion damping in a self-consistent fashion.[21] We adopt here the dielectric function proposed by Mermin [$\epsilon^{\mathrm{M}}(q,\omega)$] to describe the full nonlocal contribution of valence electrons (see the Supporting Information). This function has the desirable $q \to 0$ limit $\epsilon^{\mathrm{M}}(0,\omega) = \epsilon^{\mathrm{D}}(\omega)$. The resulting nonlocal permittivity of the metal is thus approximated by[22]

$$\epsilon(q,\omega) = \epsilon^{\mathrm{loc}}(\omega) - \epsilon^{\mathrm{D}}(\omega) + \epsilon^{\mathrm{M}}(q,\omega) \qquad (3)$$

where $\epsilon^{\mathrm{loc}}(\omega)$ is the local, frequency-dependent part of the response, taken from optical measurements.[18] We correct the latter in eq 3 by subtracting the local valence-electrons contribution ϵ^{D} and adding the nonlocal valence-electrons response ϵ^{M}. Finally, ω_p and η are chosen to fit both the long-wavelength tail and the observed plasmon frequency of ϵ^{loc} taken from refs 18 and 23 ($\hbar\omega_p = 9$ eV and $\hbar\eta = 0.05$ eV for gold; $\hbar\omega_p = 9.1$ eV and $\hbar\eta = 0.02$ eV for silver).

The momentum and distance dependence of the response of bulk gold is represented in Figure 2. In particular, Figure 2a shows the so-called loss function of gold [$\mathrm{Im}\{-1/\epsilon(q,\omega)\}$] under the approximation of eq 3, which is directly accessible to electron energy-loss spectroscopy.[24] Nonlocal effects become dramatic in the optical region for $q \gtrsim 1$ nm^{-1} (i.e., to the left

of the Landau cutoff for excitation of valence electron−hole pairs, $\omega = qv_F$), and although this is a large value compared to the momentum of light (e.g., 0.015 nm^{-1} at 3 eV), it is small compared to the inverse of some relevant distances involved in plasmonic structures. Actually, the real-space response V^{nonloc} obtained from the Fourier transform of $4\pi/[q^2\epsilon(q,\omega)]$ differs considerably from the local approximation $V^{\text{loc}} = 1/[r\epsilon^{\text{loc}}(\omega)]$ up to distances above ~1 nm [Figure 2b]. The ratio between these two quantities has a real part significantly smaller than 1 over that range of distances, while the imaginary part lies below 0.2 in modulus within the area explored in Figure 2b. This means that the short-distance interaction between induced charges will be weaker than in a locally described metal, and therefore, we should expect a softening of characteristic effects attributed to narrow gaps between metals or sharp tips (e.g., smaller red shifts). Moreover, nonlocality can be amplified by the prominent role played by tips and gaps in metallic nanostructures, because the electromagnetic field undergoes large enhancement in their vicinity. It should also be noticed that narrow gaps and sharp tips usually involve highly evanescent fields, that is, large values of q, which are more sensitive to nonlocal effects. This explanation differs from the electron collision-rate argument used in eq 1. The latter yields an excellent phenomenological description of plasmon broadening in small particles, but the physical nature of this effect seems to be more connected to the relevant role played by large q components.

III. Nonlocal Effects in Nanostructures

The presence of boundaries breaks the translational symmetry of homogeneous materials and requires some extra ingredient to be accounted for. This extra ingredient is conveniently provided by the SRM, which we use throughout this work because it can be easily implemented in arbitrarily complex geometries (see Figure 3). In the SRM, each interface separating two homogeneous media is described by surface charge distributions on either side. These surface charges contribute to *boundary* fields as if they were surrounded by an infinite nonlocal homogeneous medium (Figure 3). The surface charges are determined by imposing the continuity of the electric potential and the normal displacement across the interface.[17] The response of the inhomogeneous system is thus derived from the knowledge of nonlocal bulk dielectric functions of the materials involved.

A. Gold Spheres. It is useful to apply this formalism to spherical particles, the optical response of which is conveniently described by their multipolar response to external potentials of radial dependence r^l, which develop an induced potential $-\alpha_l/r^{l+1}$, where l is the orbital momentum number and α_l is the polarizability of order l. Applying the SRM, one finds[16]

$$\alpha_l = a^{2l+1}\frac{l\epsilon_l - l\epsilon_h}{l\epsilon_l + (l+1)\epsilon_h} \tag{4}$$

where

$$\frac{1}{\epsilon_l} = \frac{2a\,(2l+1)}{\pi}\int_0^\infty \frac{dq}{\epsilon(q,\omega)} j_l^2(qa)$$

a is the particle radius, ϵ_h is the permittivity of the local host medium surrounding the particle, and j_l is the spherical Bessel function of order l. For local media, one has $\epsilon_l = \epsilon$.

Figure 1 shows excellent agreement between the present nonlocal calculations (dashed curves) and experimental data[3] (solid curves) for light scattering by small gold particles. The calculated spectra have been shifted 15 nm to the red in order to compensate unknown factors such as metal diffusion into the dielectric, particle faceting, and other interband transitions in the dielectric.[26] Experimental spectra have been normalized by a common multiplicative factor to fit the calculated cross section. The relative shift and broadening of the observed extinction spectra are well reproduced by the calculated cross section, as it should in the small-concentration limit. The experimental curves have wider long-wavelength tails, generally resulting from finite size and shape distribution of the particles.[2] Quite different from the size-independent spectral profiles predicted by a local description, nonlocal effects give rise to significant broadening for particle radius below 2 nm [cf. Figure 2b]. These are the so-called quantum confinement effects, which show up when the mean free path of valence electrons is comparable to the particle diameter.[3] This agreement between experiment and theory supports our approach to describe nonlocal metal behavior at short distances.

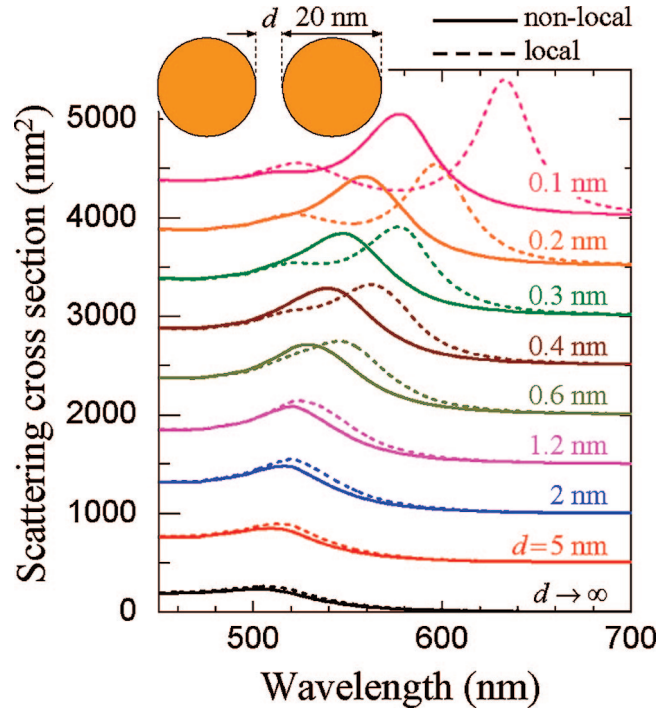

Figure 4. Extinction spectra of dimers formed by spherical gold particles of 20 nm in diameter. Local (dashed curves) and nonlocal (solid curves) calculations are compared for several separations between the particle surfaces, d. Consecutive curves are offset vertically by 500 nm^2 for clarity. The external electric field is parallel to the interparticle axis.

B. Metallic Dimers. A first example of the blue shift produced by nonlocality is shown in Figure 4 for light extinction spectra of gold dimers calculated with (solid curves) and without (dashed curves) inclusion of nonlocal effects. The shift becomes more apparent as the interparticle distance is reduced. A sizable plasmon broadening is also observed. This lowest-order longitudinal dipole mode of the dimer involves huge piling up of induced charge in the particle junction region,[8] thus enhancing the role of nonlocality.

The results of Figure 4 are obtained by describing each sphere by the multipolar polarizabilities of eq 4 and by performing multiple scattering to obtain the self-consistent field,[27] including all multipoles with $l \leq 20$, in order to achieve convergence.

The dependence of the lowest-order longitudinal dipole-mode wavelength on interparticle separation in gold and silver dimers is shown in Figure 5 with (solid curves) and without (dashed curves) inclusion of nonlocal effects. Besides significantly blue

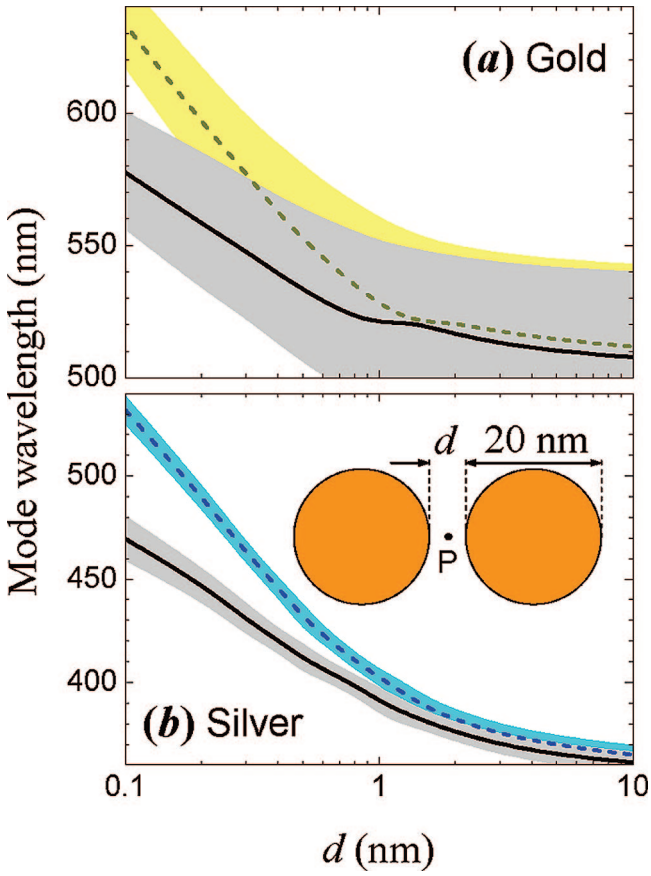

Figure 5. Dimer dipole−plasmon wavelength as a function of interparticle surface spacing d for gold (a) and silver (b) 20 nm nanoparticles. Solid and dashed curves correspond to nonlocal and local descriptions of the metal, respectively. The width of the modes is represented by shaded regions covering the fwhm span of the scattering-cross-section plasmon peaks.

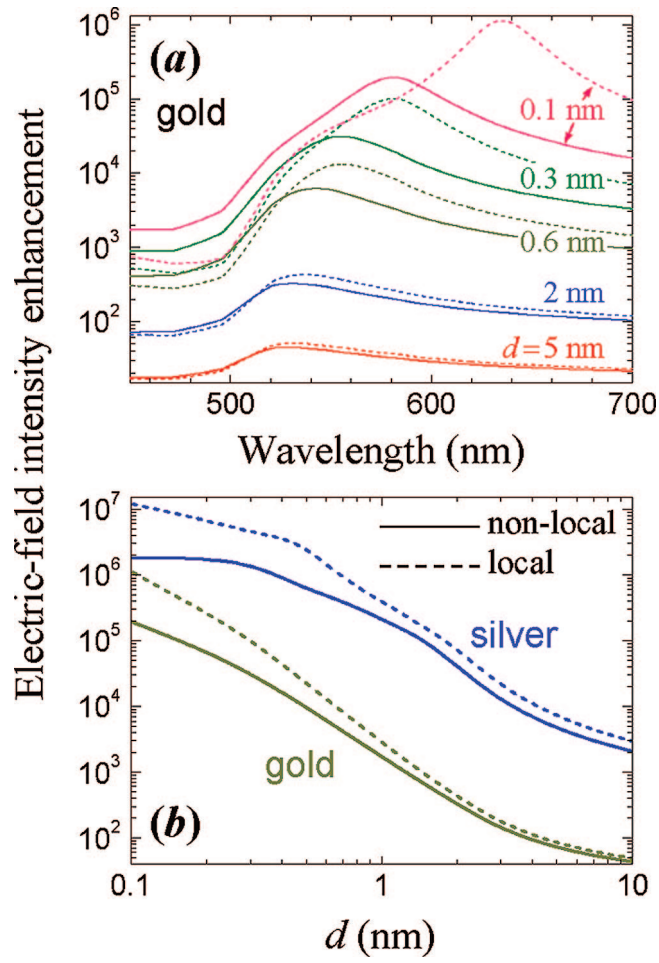

Figure 6. Enhancement of the electric field intensity relative to the incident field ($|E/E^{ext}|^2$) at the center of metallic dimers with the same dimensions as in Figure 5 (see point P in the inset of Figure 5). (a) Spectral dependence of the enhancement for various separations between the surfaces of 20-nm spherical gold particles. (b) Maximum field enhancement as a function of separation for gold and silver dimers. The results from local and nonlocal descriptions of the response are shown by dashed and solid curves, respectively.

shifting the plasmon resonance, nonlocality increases plasmon broadening (the shaded areas in the figure have a vertical width equal to the full width at half maximum (fwhm) of the plasmon resonance), an effect that we attribute to the availability of additional loss channels (valence electron−hole pairs) in the metallic response.

Actually, Figure 2 provides the key for understanding these nonlocal effects: the interaction is strongly screened at small distances due to both valence electron polarization in the region to the left of the Landau cutoff and electron−hole pair excitation to the right [see Figure 2a], thus reducing the magnitude of the effective dielectric function that induced charges experience at small separations and, therefore, resulting in larger effective separation between particles (i.e., smaller red shift, or equivalently, a blue shift).

Accompanying the far-field phenomenology discussed above, the near field is also influenced by nonlocal effects, which can reduce the field enhancement at the center of a dimer by nearly an order of magnitude, as shown in Figure 6. This limits the applicability of metal structures to SERS and nonlinear optics, as compared with the expectations opened by the field enhancement predicted in the local approximation. Again, losses originating in electron−hole pair excitations contribute to this reduction and so does the finite penetration of the induced charge toward the interior of the metal by a distance $\sim v_F/\omega$[17] (see Figure 2). This is in contrast to the vanishing penetration associated to local descriptions.

C. Thin Shells and Waveguides. Nonlocal effects are not exclusive of small particles or interparticle gaps. They are also important in other strongly interacting metallic geometries typically encountered in plasmonics, such as nanoshells [Figure 7a] and waveguides [Figure 7b]. In particular, a recent SRM account of nonlocal effects has been shown to limit the focusing properties of Pendry's thin-metal lens[28] to a maximum resolution of 5 nm.[29] Similar to dimers, the plasmon modes in these structures undergo blue shifts exceeding 10% at thicknesses below 5 Å. Interestingly, the mutually complementary geometries of the dielectric gap and the metal film considered in Figure 7b should yield the same dispersion relation in the nonretarded limit (dashed curve), but nonlocal effects produce different dispersion relations for each of these systems.

IV. Conclusions

In summary, we have shown that nonlocal effects are relevant in the response of metal systems involving short distances below a few nanometers. In particular, we have reported large blue shifts and reduced near-field intensity compared to a local description in metallic dimers, nanoshells, and thin films. These effects should be important in the design of plasmonic elements on the nanometer scale, for which the formalism introduced here provides a suitable and versatile framework that can find general applicability in nanoparticles and other nanostructures of arbitrary morphology.

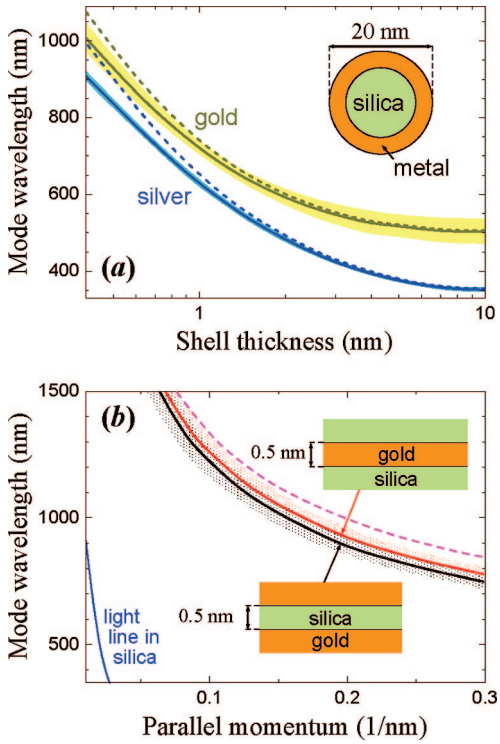

Figure 7. (a) Dipolar mode wavelength of gold and silver shells surrounding a silica core ($\epsilon = 2.1$) as a function of metal thickness. Solid and dashed curves correspond to nonlocal and local descriptions of the metal, respectively. The width of the modes is represented through shaded regions covering the fwhm span of the scattering-cross-section plasmon peaks. (b) Plasmon dispersion relations in gold−silica−gold and silica−gold−silica waveguides for a 0.5-nm thick central layer. The nonlocal description (solid curves) produces different results for these mutually complementary geometries, in contrast to the local description (dashed curve).

More elaborate methods have also been used to describe nonlocality, particularly using density-functional theory[12,30] and plasmon quantum models,[31] although they become impractical in large systems or non trivial geometries. In contrast, the SRM used here accounts for the main features of nonlocality and is sufficiently versatile to deal with relatively complex systems like those discussed above. Our results are important to design plasmon resonances in nanometer metallic elements with application to optical antennas, as well as for improved photovoltaic, lighting, and sensing devices.

Acknowledgment. I would like to thank Javier Aizpurua, Jeremy Baumberg, Peter Nordlander, and Mark Stockman for fruitful discussions. This work was supported by the Spanish MEC (NAN2004-08843-C05-05, MAT2007-66050, and Nano-Light.es consolider) and by the EU-FP6 (NMP4-2006-016881 "SPANS").

Supporting Information Available: Lindhard and Mermin dielectric functions. This material is available free of charge via the Internet at http://pubs.acs.org.

References and Notes

(1) Bohren, C. F.; Huffman, D. R. *Absorption and Scattering of Light by Small Particles*; Wiley-Interscience: New York, 1983.
(2) Myroshnychenko, V.; Rodríguez-Fernández, J.; Pastoriza-Santos, I.; Funston, A. M.; Novo, C.; Mulvaney, P.; Liz-Marzán, L. M.; García de Abajo, F. J. *Chem. Soc. Rev.* **2008**, *37*, 1792–1805.
(3) Kreibig, U.; Vollmer, M. *Optical Properties of Metal Clusters*; Springer-Verlag: Berlin, 1995.
(4) Danckwerts, M.; Novotny, L. *Phys. Rev. Lett.* **2007**, *98*, 026104.
(5) Prodan, E.; Radloff, C.; Halas, N. J.; Nordlander, P. *Science* **2003**, *302*, 419–422.
(6) Kumar, P. S.; Pastoriza-Santos, I.; Rodríguez-González, B.; García de Abajo, F. J.; Liz-Marzán, L. M. *Nanotechnology* **2008**, *19*, 015606.
(7) Li, K. R.; Stockman, M. I.; Bergman, D. J. *Phys. Rev. Lett.* **2003**, *91*, 227402.
(8) Romero, I.; Aizpurua, J.; Bryant, G. W.; García de Abajo, F. J *Opt. Express* **2006**, *14*, 9988–9999.
(9) Xu, H.; Bjerneld, E. J.; Käll, M.; Börjesson, L. *Phys. Rev. Lett.* **1999**, *83*, 4357–4360.
(10) Derkacs, D.; Lim, S. H.; Matheu, P.; Mar, W.; Yu, E. T. *Appl. Phys. Lett.* **2006**, *89*, 093103.
(11) Mertens, H.; Biteen, J. S.; Atwater, H. A.; Polman, A. *Nano Lett.* **2006**, *6*, 2622–2625.
(12) Idrobo, J. C.; Walkosz, W.; Yip, S. F.; Ögüt, S.; Wang, J.; Jellinek, J. *Phys. Rev. B* **2007**, *76*, 205422.
(13) Feibelman, P. J. *Prog. Surf. Sci.* **1982**, *12*, 287–407.
(14) Ritchie, R. H.; Marusak, A. L. *Surf. Sci.* **1966**, *4*, 234–240.
(15) Wagner, D. *Z. Naturforsch. A* **1966**, *21*, 634.
(16) (a) Dasgupta, B. B.; Fuchs, R. *Phys. Rev. B* **1981**, *24*, 554–561. (b) Fuchs, R.; Claro, F. *Phys. Rev. B* **1987**, *35*, 3722–3727. (c) Rojas, R; Claro, F.; Fuchs, R. *Phys. Rev. B* **1988**, *37*, 6799–6807.
(17) García de Abajo, F. J; Echenique, P. M. *Phys. Rev. B* **1992**, *46*, 2663–2675. *Phys. Rev. B* **1993**, *48*, 13399−13407.
(18) Johnson, P. B.; Christy, R. W. *Phys. Rev. B* **1972**, *6*, 4370–4379.
(19) It is customary to introduce an extra multiplicative parameter A in the Av_F/a effective collisional rate that depends on size and particle environment and that is used to fit experimental observations. See Pinchuk, A.; Kreibig, U.; Hilger, A. *Surf. Sci.* **2004**, *557*, 269–280, and references therein.
(20) Lindhard, J. K. *Dan. Vidensk. Selsk. Mat. Fys. Medd.* **1954**, *28*, 8.
(21) Mermin, N. D. *Phys. Rev. B* **1970**, *1*, 2362–2363.
(22) In a more systematic derivation to be published elsewhere, eq 3 is the response function of a noninteracting electron gas with the density of valence electrons of our metal, and in the presence of an ionic background described by a local dielectric function, which is chosen to fit the measured permittivity in the $q = 0$ limit.
(23) The values of ω_p obtained for gold and silver agree nicely with the ones expected from the density of s valence electrons.[18]
(24) Batson, P. E.; Silcox, J. *Phys. Rev. B* **1983**, *27*, 5224–5239.
(25) García-Moliner, F.; Flores, F. *Introduction to the Theory of Solid Surfaces*; Cambridge University Press: Cambridge, 1979.
(26) Pinchuk, A.; von Plessen, G.; Kreibig, U. *J. Phys. D: Appl. Phys.* **2004**, *37*, 3133–3139.
(27) García de Abajo, F. J. *Phys. Rev. B* **1999**, *60*, 6086–6102.
(28) Pendry, J. B. *Phys. Rev. Lett.* **2000**, *85*, 3966–3969.
(29) Larkin, I. A.; Stockman, M. I. *Nano Lett.* **2005**, *5*, 339–343.
(30) Prodan, E.; Nordlander, P.; Halas, N. J. *Nano Lett.* **2003**, *3*, 1411–1415.
(31) Prodan, E.; Nordlander, P.; Halas, N. J. *Chem. Phys. Lett.* **2003**, *368*, 94–101.

JP807345H

Nonlocal Effects in the Plasmons of Strongly Interacting Nanoparticles, Dimers, and Waveguides - Supplementary Information

F. Javier García de Abajo*
Instituto de Óptica - CSIC, Serrano 121, 28006 Madrid, Spain
(Dated: October 8, 2008)

Lindhard Dielectric Function

The conduction band of good metals such as aluminum, silver, and gold can be described as a gas of non-interacting free electrons.[1] The dielectric function of such a system is obtained by perturbing the plane-wave representing each electron within the Fermi sphere by means of an external potential of the form $\phi^{\rm ext} = \exp({\rm i}\mathbf{q}\cdot\mathbf{r} - {\rm i}\omega t)$. The sum of these perturbations for all conduction electrons produces an induced charge $\rho^{\rm ind}$ proportional to $\phi^{\rm ext}$. The system is then assumed to be perturbed by the self-consistent total potential rather than the induced potential in what is called the random-phase approximation (RPA), which leads to the following expression for the dielectric function:[1]

$$\epsilon(q,\omega) = \left[1 + \frac{4\pi}{q^2}\frac{\rho^{\rm ind}}{\phi^{\rm ext}}\right]^{-1} = 1 + \frac{e^2}{\pi^2\hbar q^2}\int d\mathbf{k}\,\frac{f_{\mathbf{k}-\mathbf{q}/2} - f_{\mathbf{k}+\mathbf{q}/2}}{\hbar\,\mathbf{k}\cdot\mathbf{q}/m + \omega},$$

where m and e are the electron mass and charge, respectively, the integral is extended over 3D electron wavevectors $\mathbf{k}$, f_k is the Fermi distribution (approximately 1 for $k \le k_F$ and 0 otherwise at room temperature), and $k_F = mv_F/\hbar$ is the Fermi wavevector. This integral was solved explicitly by Lindhard[2] to find the closed expression

$$\epsilon^L(q,\omega) = 1 + \frac{2me^2k_F}{\pi\hbar^2q^2}\left[1 + R(x,y) + R(x,-y)\right],$$

where $x = q/k_F$, $y = \hbar\omega/E_F$, $E_F = \hbar^2k_F^2/2m$ is the Fermi energy, and

$$R(x,y) = \frac{1}{2x}\left[1 - \left(\frac{x^2+y}{2x}\right)^2\right]\log\left(\frac{x^2+2x+y}{x^2-2x+y}\right).$$

Here, ω is assumed to have a positive imaginary part. If $\mathrm{Im}\{\omega\}$ is infinitesimally small then $\mathrm{Im}\{\epsilon^L(q,\omega)\}$ takes nonzero values only for $x(x-2) \le y \le x(x+2)$ (i.e., in the so-called electron-hole region).

Mermin Dielectric Function

A naive way of introducing a finite damping rate η in the electron-gas motion consists in adding a finite imaginary part to ω, but this results in a net loss of the number of electrons with time. The Lindhard formula was extended by Mermin[3] to include finite damping while maintaining the number of electrons constant. He found the expression

$$\epsilon^M(q,\omega) = 1 + \frac{(\omega+{\rm i}\eta)\left[\epsilon^L(q,\omega+{\rm i}\eta) - 1\right]}{\omega + {\rm i}\eta\left[\epsilon^L(q,\omega+{\rm i}\eta) - 1\right]/\left[\epsilon^L(q,0) - 1\right]},$$

where

$$\epsilon^L(q,0) = 1 + \frac{2me^2k_F}{\pi\hbar^2q^2}\left[1 + \frac{4-x^2}{4x}\log\left|\frac{x+2}{x-2}\right|\right]$$

is the static limit of ϵ^L.

---

* Electronic address: jga@cfmac.csic.es

[1] Ashcroft, N. W.; Mermin, N. D. *Solid State Physics;* Harcourt College Publishers: New York, 1976.
[2] Lindhard, J. *K. Dan. Vidensk. Selsk. Mat. Fys. Medd.* **1954,** *28,* no. 8.
[3] Mermin, N. D. *Phys. Rev. B* **1970,** *1,* 2362–2363.